Physica Medica 63 (2019) 41–47

Contents lists available at ScienceDirect

Physica Medica

journal homepage: www.elsevier.com/locate/ejmp

Original paper

Beam focal spot intrafraction motion and gantry angle dependence: A study of Varian linac focal spot alignment

Luke A. Slama[a,b,*], Hans L. Riis[c], Mahsheed Sabet[b], Michael P. Barnes[d,e,f], Martin A. Ebert[a,b], Sun Chan[g], Pejman Rowshanfarzad[a]

[a] Department of Physics, the University of Western Australia, Crawley, WA, Australia
[b] Department of Radiation Oncology, Sir Charles Gairdner Hospital, Nedlands, WA, Australia
[c] Radiofysisk Laboratorium, Odense University Hospital, DK-5000 Odense C, Denmark
[d] Department of Radiation Oncology, Cavalry Mater Newcastle, Newcastle, NSW, Australia
[e] School of Health Sciences, University of Newcastle, Newcastle, NSW, Australia
[f] School of Mathematical and Physical Sciences, University of Newcastle, Newcastle, NSW, Australia
[g] Department of Medical Technology and Physics, Sir Charles Gairdner Hospital, Nedlands, WA, Australia

ARTICLE INFO

Keywords:
Focal spot
Quality assurance
Varian
Commissioning

ABSTRACT

The characteristics of the focal spot of the linear accelerator (linac) play a role in determining the resulting dose distribution within the patient, and hence probability of treatment success. A direct measurement of focal spot position is not recommended by AAPM Task Group 142, but factors influenced by focal spot position, such as beam symmetry and isocentre position, are. Traditional methods of measuring focal spot position are time consuming and can only be performed at gantry 0°. The presented method has been proposed using a phantom of novel design to accurately measure the position of the focal spot relative to the collimator's axis of rotation (CAX) at any gantry angle, and to measure the intra-fraction movement of the focal spot relative to the mean position during treatment. The method was reproducible to within 0.012 mm/0.029 mm (mean/max) for the three Varian linacs tested. The focal spot position was shown to deviate from the CAX by up to 0.386 mm during gantry rotation. The focal spot position was more unstable at the start of treatment, with the worst performing linac having an initial displacement of up to 0.15 mm from its mean position before stabilizing to within 0.01 mm after 3 s. The method proposed is a beneficial addition to the quality assurance (QA) schedule of any clinic, allowing quick determination of source position and movement at any gantry angle. Measurement of focal spot allows the possibility of fine-tuning the electron beam steering system to improve the standard of the photon beam and of stereotactic treatments.

1. Introduction

Highly accurate treatment machines are required for modern radiotherapy techniques where a high geometric accuracy is desired. On clinical C-arm linacs, the geometric intersection of the rotation axes of the couch, gantry and beam collimation system is known as the mechanical isocentre, and the geometric intersection of the central axis of all radiation beams through linac motion is known as the radiation isocentre. The shape, size and position of the mechanical isocentre [1–4] can be influenced by gantry sag [3,5–9], gantry head tilt and inaccuracies in the precision bearing system [3,10–12].

The radiation isocentre is meant to coincide with the mechanical isocentre and is influenced by the mechanical isocentre, collimation positional inaccuracies including sag [13], focal spot position misalignment with the CAX and a misalignment of the treatment beam and flattening filter with the collimators' central axis (CAX) [14–17]. The ability to independently measure each of these parameters is desirable to determine which quantity is most in error to improve isocentre accuracy.

The report of the American Association of Physicists in Medicine (AAPM) Task Group 142 [18] recommends that maximum runout of each axis (size of the isocentre), and the coincidence of radiation and mechanical isocentre should be no more than 1 mm for stereotactic radiosurgery (SRS) or stereotactic body radiotherapy (SBRT), and no more than 2 mm for non-SRS treatment machines.

Numerous methods have been proposed for measuring linac isocentre positions including use of mechanical pointers [19] or Varian's IsoLock method [20] for the mechanical isocentre, starshot tests

* Corresponding author at: Department of Radiation Oncology, B Block, Sir Charles Gairdner Hospital, Hospital Ave, Nedlands, WA 6009, Australia.
E-mail address: Luke.Slama@health.wa.gov.au (L.A. Slama).

https://doi.org/10.1016/j.ejmp.2019.05.021
Received 30 December 2018; Received in revised form 2 May 2019; Accepted 25 May 2019
Available online 29 May 2019
1120-1797/ © 2019 Published by Elsevier Ltd on behalf of Associazione Italiana di Fisica Medica.

[1,7,11,21,22] for the radiation isocentre, Winston-Lutz tests [3,23,24] for the coincidence of the mechanical and radiation isocentres, and Varian's IsoCal method [25] to validate the coincidence of the radiation and imaging isocentres.

The focal spot position is the position on the tungsten target at which the electron beam strikes to produce the clinical photon radiation beam. This should be aligned with CAX to ensure maximum treatment accuracy. The position, size and shape of the focal spot are largely dependent on the beam steering and servo systems, consisting of various focussing and deflection coils. A dual monitoring system and feedback control loop increase the accuracy of the focal spot position by monitoring beam symmetry and adjusting various steering coils to correct for any asymmetry. Varian machines steer for electron beam angle, with a servo system connected to two D shape ion chambers as part of the monitoring system and adjusting the transverse and radial angle coil currents. Two C shaped ion chamber monitoring chambers that are connected to a servo system controlling the radial and transverse steering coils to change the focal spot translational position and increase beam symmetry [26]. At the treatment level, the radial coils primarily affect the treatment beam in the in-plane direction, and the transverse coils affect the beam in the cross-plane direction.

Nyiri et al. [15] proposed two methods to determine focal spot position. The corotational penumbra modulation method is sensitive to jaw sag and thus can only be performed at gantry 0° [27]. The image centre shift method consists of taking images at multiple collimator angles of two rod phantoms attached to a specially-made jig at different distances from the source. This was only performed at gantry 0°.

Chojnowski et al. [28] proposed a phantomless method utilising the jaws and MLC, taking four images of a $10 \times 10\,cm^2$ field at opposed collimator angles. This method is fast in determining focal spot misalignment, but is dependent on jaw sag and so is limited to gantry 0°. Barnes et al. [29] extended the work of Chojnowski et al. to implement an EPID based method of angular and translational beam steering of Varian linacs. This method is much faster than traditional methods of beam steering, but can only be performed at gantry 0°.

Yuen et al. [17] developed and tested a phantom designed to attach to the linac accessory mount and perform a focal spot position test similar to the half beam block method. The method was shown to be highly accurate with a 0.01% standard uncertainty, but was only performed at gantry 0°.

Sonke et al. [30] measured the intra-fraction movement of the focal spot by taking images of a rod phantom in continuous acquisition or movie mode. This method was only performed at gantry 0°, and measures the focal spot position at the isocentre level.

The traditional method of measuring focal spot position is done using half beam blocking [31], but is usually not done routinely due to the large amount of time required. Jaw sag influences this method, and thus can only be performed at gantry 0°.

This study aims to introduce a novel method to determine the focal spot position of linear accelerators relative to the CAX at the source level. Unlike previous methods, this method can be performed at any gantry angle due to the stability of the phantom used. The phantom is also used to measure intra-fraction movement of the focal spot relative to its mean position, at multiple gantry angles. Although the method can be applied to any linac, the present work only focusses on Varian linacs.

2. Materials and methods

2.1. Accelerators and EPIDs

One Varian Trilogy linac, one Varian Clinac iX linac, and two Varian TrueBeam linacs (Varian Medical Systems, Inc. Palo Alto, CA, USA) were used to acquire data. Due to the similarities in construction, the Trilogy and Clinac iX will henceforth be known as Clinacs when referring to both these machines, and as Trilogy or iX when referring to the individual machine. The TrueBeams will be labelled as TrueBeam A and TrueBeam B. The iX and the TrueBeams are used for SRS, Intensity Modulated Radiotherapy (IMRT) and Volumetric Modulated Arc Therapy (VMAT) treatments. The Clinacs are capable of 6MV and 18MV photon treatment modalities, and the TrueBeam is equipped with 6MV, 10MV and 6MV flattening filter free (FFF) treatment modes.

An a-Si 1000 digital electronic portal imaging device (EPID) panel installed on each linac was used to acquire the images with a panel resolution of 0.391 mm.

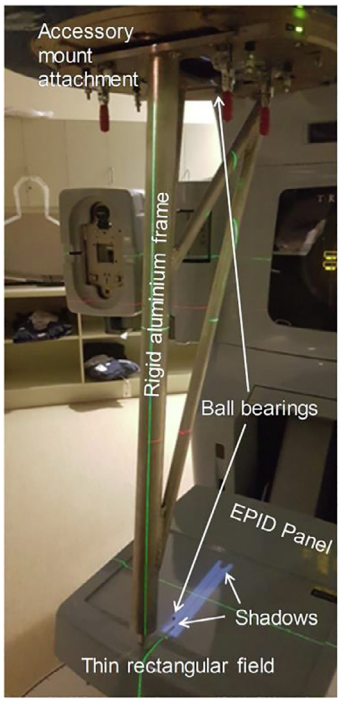

Fig. 1. Focal spot phantom attached to the treatment head of a Varian Trilogy, with field light and EPID showing initial setup position. The ball bearings are located at the top and bottom of the phantom, with projected shadows at each end of the thin field.

2.2. Phantom design and function

A specialized phantom was developed to attach to Varian linac heads using the same concept as for Elekta linacs[32] (Fig. 1). The phantom consists of two tungsten ball bearings housed on a rigid aluminium frame, with a base plate designed to attach to the accessory mount of the linac. One ball bearing is positioned close to the exit window, and the other to the EPID panel. Both are placed at opposite ends of the treatment field to avoid interference in the images. The phantom weighs 4.619 kg and simulations using SOLIDWORKS Simulation software (2013 SP4.0) indicated a maximum deflection of 0.01–0.02 mm at any gantry angle. The ball bearings have diameters of 4.75 mm and 6.35 mm.

The field is shaped as a thin rectangle with the ball bearing shadows on either end along the long axis, with a field size of $4 \times 16\,cm^2$ at the source-axis distance (SAD). The collimator is then rotated, and images taken at 12 different collimator angles spaced equally by 30°.

An illustration of the method is shown in Fig. 2. Both ball bearings will rotate around CAX and, assuming the focal spot is aligned with CAX, will produce radiation-beam shadows centred about CAX. Any shift from CAX is due to a misalignment of the focal spot. This shift is dependent upon the focal spot position relative to CAX at the source level, $\vec{d}$, source to ball bearing distances, l_1 and l_2, and the source to detector distance, l_3.

The centre of the circles traced out by the ball bearing shadows are

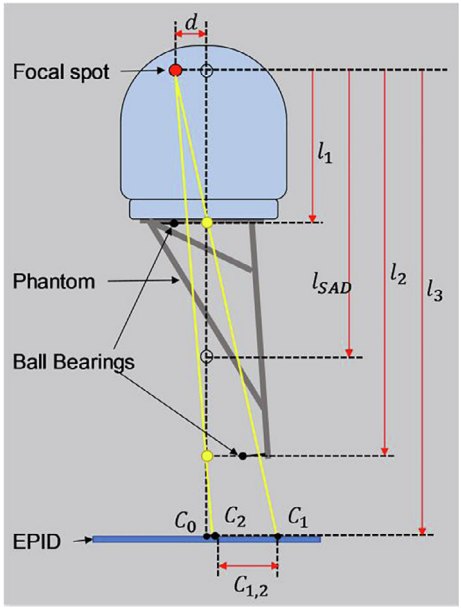

Fig. 2. The centres of the circles traced out by the ball bearing shadows have positions, $\vec{C}_1$ and $\vec{C}_2$, that are a projection from the focal spot (red circles), through the centre of rotation of the ball bearings or CAX (yellow circles), to the EPID panel (yellow lines). The displacement, $\vec{d}$, of the focal spot from the CAX, $\vec{C}_0$, or expected focal spot position, will affect the shadow positions of the upper ball bearing at l_1 more than the ball bearing at l_2. The difference in these projections, $\vec{C}_{1,2}$, can be used to determine $\vec{d}$ using Eq. (2).

at $\vec{C}_1$ and $\vec{C}_2$ for the upper and lower ball bearings respectively. The centre of rotation, or CAX, at $\vec{C}_0$ can be determined by Eq. (1).

$$\vec{C}_0 = \vec{C}_1 + \vec{d}\left(1 - \frac{l_3}{l_1}\right) = \vec{C}_2 + \vec{d}\left(1 - \frac{l_3}{l_2}\right) \quad (1)$$

Rearranging this equation, we can eliminate $\vec{C}_0$ to determine $\vec{d}$ by Eq. (2), where $\vec{C}_{1,2}$ is $\vec{C}_2$ -$\vec{C}_1$. We can then substitute the value of $\vec{d}$ into Eq. (1) to find $\vec{C}_0$.

$$\vec{d} = \frac{l_1 l_2}{l_3(l_2 - l_1)}\vec{C}_{1,2} \quad (2)$$

A measurement of focal spot position relative to its stable position can be calculated when taking multiple images at the same gantry and collimator angle. The stable position is here defined as the mean position of the focal spot from 5 s after the beam is switched on to the end of delivery, $\vec{d}_{av}$. The distance between the two shadow positions, $\vec{S}_{1,2}$, is calculated for each image, and the mean distance across all but the first 5 s worth of images in the acquisition, $\vec{S}_{1,2,av}$ is subtracted from these. This is analogous to subtracting the mean distance between circle centres. The position of the focal spot from its stable position, $\vec{d} - \vec{d}_{av}$, can then calculated using Eq. (3).

$$\vec{d} - \vec{d}_{av} = \frac{l_1 l_2}{l_3(l_2 - l_1)}(\vec{S}_{1,2} - \vec{S}_{1,2,av}) \quad (3)$$

2.3. Computer aided software

In-house MATLAB developed software (MATLAB R2015a, The MathWorks, Inc., Natick, Massachusetts, USA) was used to analyse the images. The two ball bearing shadows are located by taking the regions of interest about the shadow and using the circular Hough transform (Fig. 3a). For the full range of collimator angles, a circle is fitted to the large (upper) and small (lower) ball bearing shadows, with centres at $\vec{C}_1$ and $\vec{C}_2$ respectively (Fig. 3b). Eq. (2) is then used to calculate the focal spot position, $\vec{d}$.

2.4. Acquisition of data

With the phantom attached to the treatment head using the accessory tray slot and 4 toggle clamps to secure the phantom in place, the EPID panel was positioned as close to the lowest point of the phantom as possible without any collisions. A series of images were acquired at 12 different collimator angles to give a single measurement of focal spot misalignment using the method described above. Field sizes of 4 cm × 16 cm were used with a source to detector distance (SDD) of 167 cm. This was repeated at 12 different gantry angles for each photon treatment modality available, producing 144 dicom image files. The measurement was repeated a total of 3 times at gantry 0° and gantry 180° to test for reproducibility. All images were taken at 100

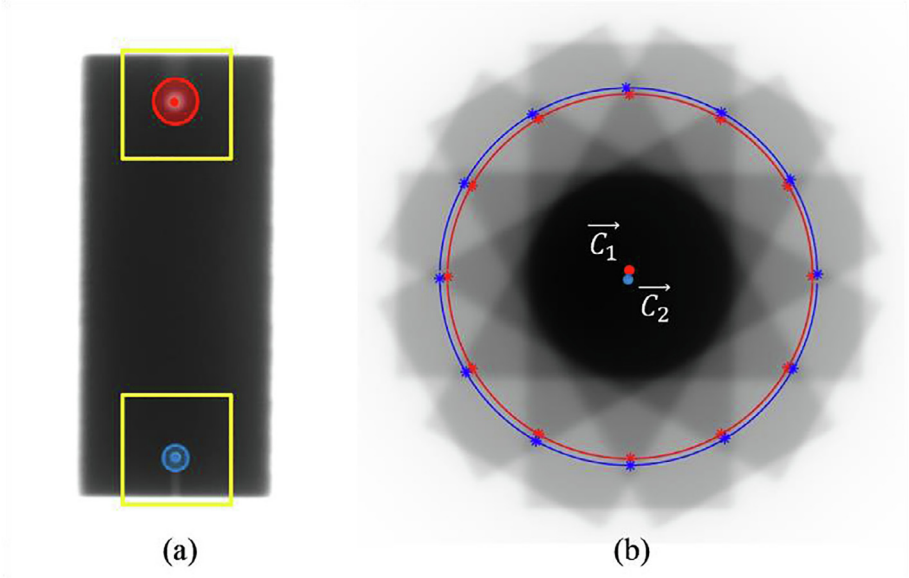

Fig. 3. The Circular Hough transform is used on the regions of interest (yellow boxes) to locate the ball bearing shadows indicated by the red and blue circles (a). A circle is fitted to the upper (red) and lower (blue) shadows across the 12 images (b), with circle centres $\vec{C}_1$ and $\vec{C}_2$ for the upper and lower shadows respectively.

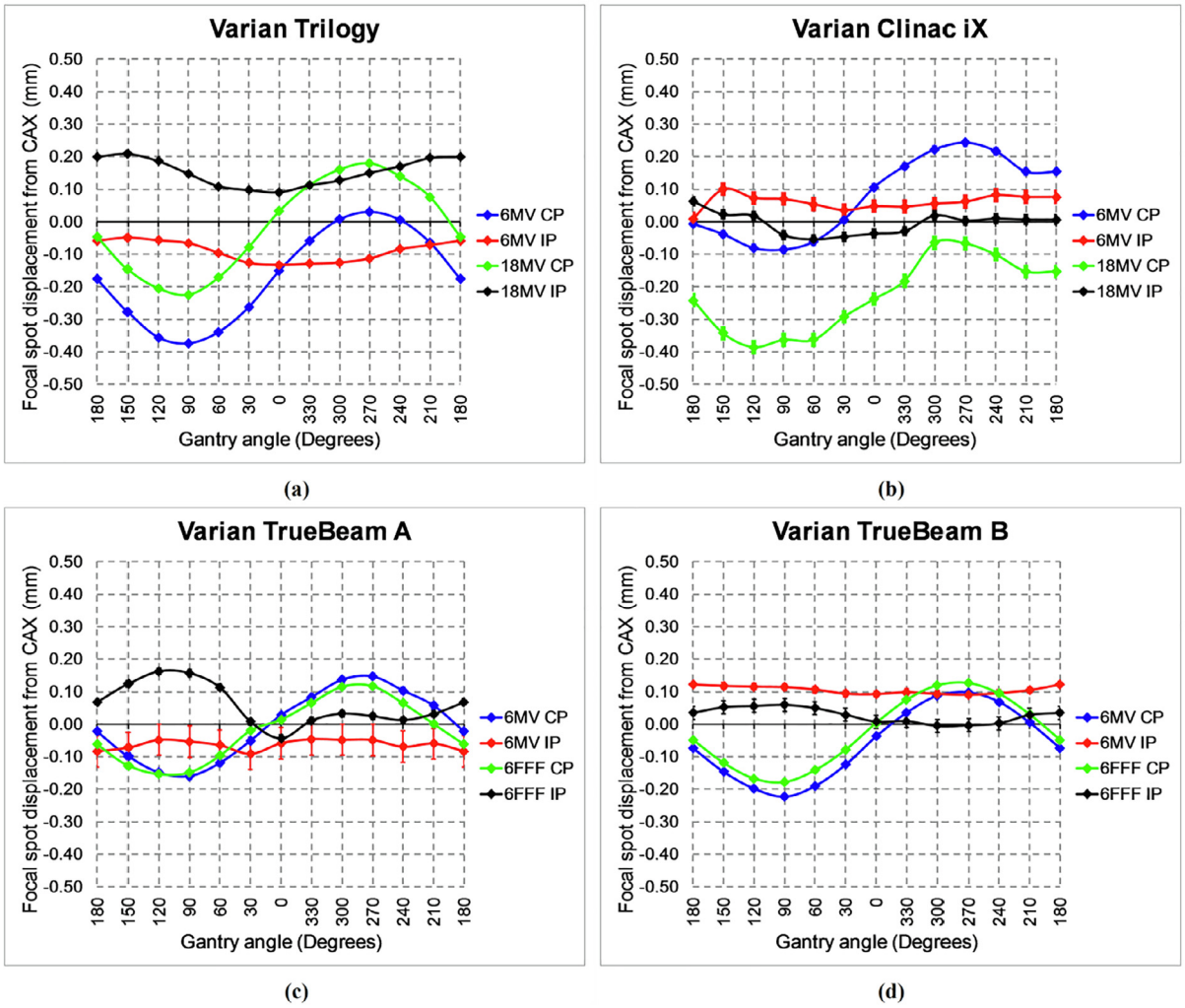

Fig. 4. The measured focal spot misalignments of the Varian Trilogy (a), Clinac iX (b), TrueBeam A (c) and TrueBeam B (d) as a function of gantry angle. Each Linac and energy combination was measured on the same day, including tests for reproducibility. CP and IP indicate cross-plane and in-plane misalignments respectively. The error bars are taken from Table 1 for each linac and energy.

Table 1
1σ reproducibility uncertainties for all linacs in mm for the cross-plane and in-plane position of the focal spot relative to CAX. The maximum reproducibility is recorded from the standard deviations calculated at gantry 0° and 180°.

Linac	Energy	Cross plane position (mm)	In plane position (mm)
Trilogy	6 MV	0.009	0.029
	18 MV	0.017	0.021
Clinac iX	6 MV	0.006	0.015
	18 MV	0.012	0.010
TrueBeam A	6 MV	0.010	0.016
	6 FFF	0.007	0.010
TrueBeam B	6 MV	0.005	0.009
	6 FFF	0.003	0.020

monitoring units (MU) per image at a dose rate of 600 MU/min for the 6 MV and 18 MV energies, and 1400 MU/min for the 6 MV FFF beam.

2.5. Comparison to an IC array measurement

To validate the accuracy of the presented method, a measurement of focal spot position was performed at Gantry 0° using an Ion chamber (IC) array (Profiler2, Sun Nuclear Corporation, Melbourne, Florida, USA) on a Varian TrueBeam to compare to the phantom measurement.

Table 2
Maximum absolute deviation of focal spot position, in mm, across all considered gantry angles, relative to CAX. The maximum recorded deviation in cross-plane and in-plane directions is recorded, as well as the maximum distance between the focal spot and the CAX.

Linac	Energy	Cross plane deviation (mm)	In plane deviation (mm)	Distance (mm)
Trilogy	6 MV	0.374	0.157	0.380
	18 MV	0.224	0.208	0.277
Clinac iX	6 MV	0.243	0.099	0.251
	18 MV	0.386	0.062	0.386
TrueBeam A	6 MV	0.160	0.091	0.169
	6 FFF	0.154	0.163	0.224
TrueBeam B	6 MV	0.223	0.122	0.251
	6 FFF	0.178	0.059	0.188

This was done by attaching the IC array to the accessory mount of the gantry, and taking measurements of the beam profile at collimator angles of 90° and 270°. The average beam centre between collimator 90° and 270° measured with the IC array is a measure of the influence of focal spot position on the beam at the measurement level [33].

The values of $\vec{C}_{1,2}$ measured using the phantom were then back projected to the IC array level by multiplying it by l_{ICA}/l_3, where l_{ICA} is

Table 3
Focal spot position measured at gantry 0° using an IC array and the presented method on Varian TrueBeam B. Three measurements were taken for each test, and the average positions recorded, in mm.

Method	Cross plane position (mm)	In plane position (mm)
IC array	−0.020	0.063
Phantom	−0.017	0.066

the SDD of the IC array in the accessory mount, 57.4 cm.

2.6. Focal spot movement during treatment

The phantom and imager were set up as described in the previous section, with gantry and collimator both at 0°. The EPID panel was then used to acquire multiple images in continuous acquisition or cine mode while the beam is running. Eq. (3) is then used to calculate the focal spot displacement from its stable position as a function of time. Images were acquired at 3 fps for the Clinacs, and 12fps for the TrueBeams. This was performed for the 6 MV and 18 MV beams on the Clinacs, and 6 MV and 6FFF for the TrueBeams, at gantry 0° and 180°. All images for this test were acquired at a dose rate of 600 MU/min for all energies, which corresponds to an exposure of 3.33 MU/image and 0.83 MU/image for the Clinacs and TrueBeams respectively.

3. Results

Plots of focal spot in-plane (IP – gun-target direction) and cross-plane (CP – orthogonal to gun-target direction) positions for each linac are shown in Fig. 4.

The reproducibility uncertainties for each linac and energy are tabulated in Table 1. The method had a mean and max reproducibility of 0.012 mm and 0.029 mm respectively (1σ). This is based on the values of the reproducibility uncertainty for the cross plane and in plane deviations of the focal spot from CAX recorded in Table 1.

The maximum displacement of the focal spot position of each linac and energy from CAX during gantry rotation is shown in Table 2. The focal spot is shown to have a maximum displacement from CAX of 0.386 mm and 0.208 mm for the cross-plane and in-plane positions respectively. This corresponds to a beam centre shift of 0.420 mm and 0.226 mm at the isocentre level for the cross-plane and in-plane positions respectively.

The measurements acquired with the IC array and phantom at gantry 0° are shown in Table 3. The results of both methods agree to within 0.003 mm.

The results of measuring focal spot position as a function of time are shown in Fig. 5. All three linacs tested are shown, for each energy and

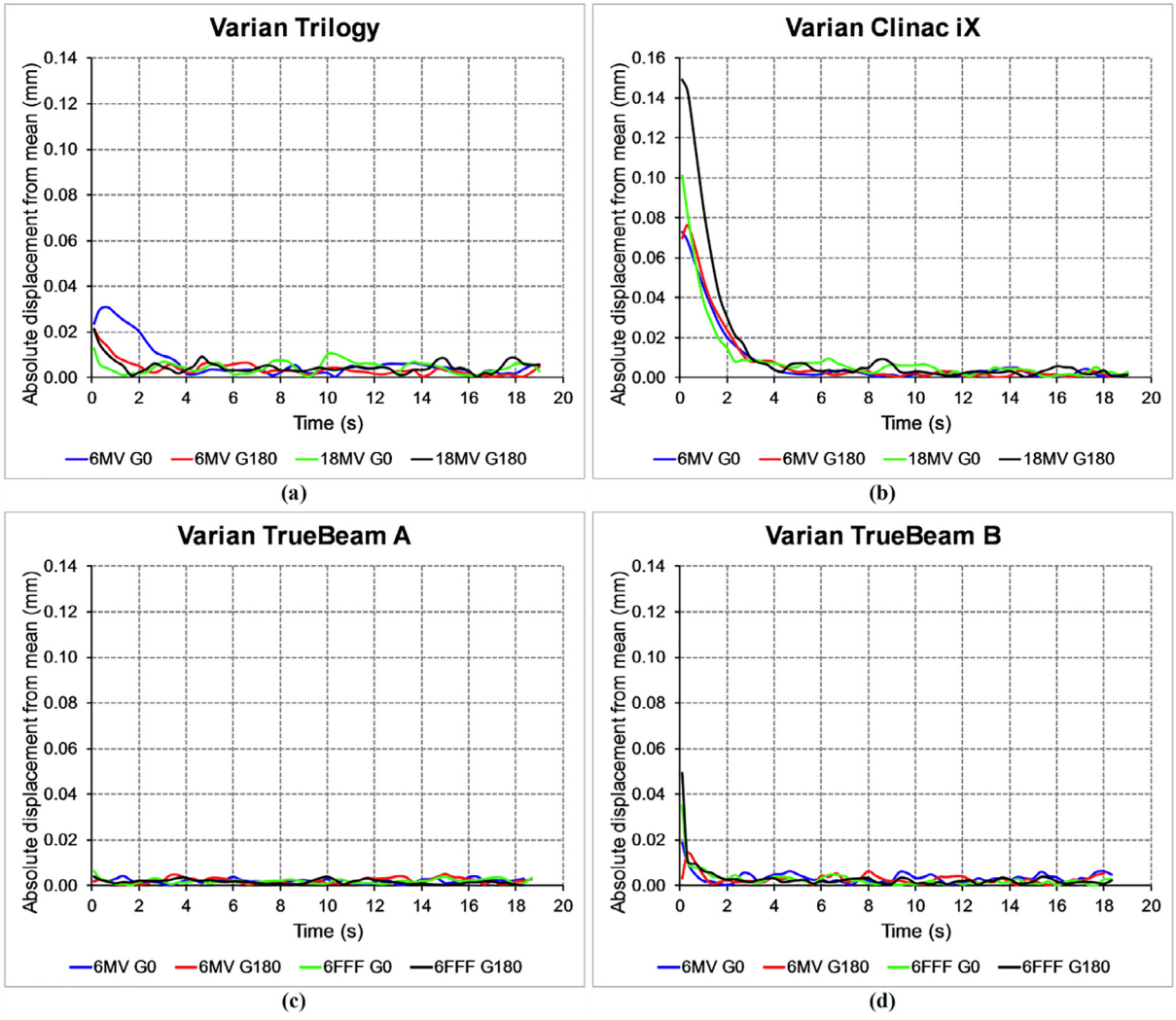

Fig. 5. Average absolute distance of the focal spot from the mean position, averaged over 3 series for the Varian Trilogy (a), Clinac iX (b), TrueBeam A (c) and TrueBeam B (d) as a function of time. Each Linac and energy combination was measured on the same day. A 5-point moving average is applied to smooth the data. The TrueBeam data was measured at 12fps and the Clinacs at 3fps, and all data is resampled to a 0.33 s temporal resolution.

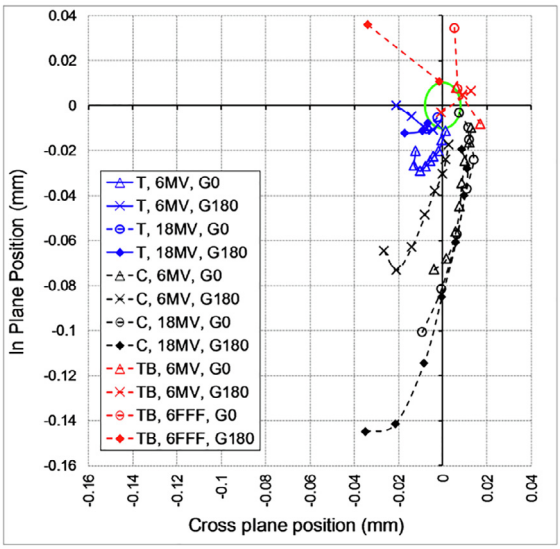

Fig. 6. Trajectory of the focal spot from its initial position to the stable position, averaged over 3 series for the Varian Trilogy (T, Blue), Clinac iX (C, Black) and TrueBeam B (TB, Red). The green ellipse represents the maximum cross plane and in plane displacement observed over all Linacs once the beam is stabilised. A 5-point moving average is applied to both the cross plane and in plane directions to smooth the data. The TrueBeam data was measured at 12fps and the Clinacs at 3fps, and resampled to a 0.33 s temporal resolution. Only the data prior to the beam stabilising is shown.

gantry angle tested. The iX showed the largest instability of up to 0.15 mm before stabilizing to within 0.01 mm after 2.5 s.

Fig. 6 shows the trajectory the focal spot takes to reach its stable position. The trajectory of both Clinacs as TrueBeam B is plotted in the figure. TrueBeam A is omitted as its focal spot is observed to have no initial focal spot instability.

4. Discussion

The method described has been shown to be successful in determining the focal spot position with a reproducibility of less than 0.012 mm/0.029 mm (mean/max) and has shown to be robust at the cardinal angles on three different models of Varian linacs. The results agree with an IC array measurement on a Varian TrueBeam at gantry 0° to within 0.003 mm.

Many methods ignore the influence of gantry rotation on linac focal spot position. This method has shown that, during a full gantry rotation, there is a deviation of focal spot position from the CAX of up to 0.386 mm at the source level, and a maximum deviation in beam centre at the isocentre level of 0.420 mm. This is 42% and 21% of the isocentre size tolerances for SRS and non-SRS treatments respectively.

For the Clinacs and TrueBeam B, the focal spot is observed to have a displacement from its mean position for the first few seconds of treatment of up to 0.15 mm, before taking an almost direct path to within 0.01 mm from the stable position after 1–3 s. This is likely due to the servo system that adjusts focal spot position as the beam is running, using measurements of beam symmetry supplied by the dual monitoring unit. The initial displacement of the focal spot is dependent on the action of the beam steering system before any adjustments by the servo system, and the time to stabilise depends on the servo period, which must account for the time to measure beam symmetry, and the time to adjust the coil currents.

There were no trends between linacs as to which gantry angle and energy was the most unstable, as the linacs were least stable under different conditions. Peak instability of all linacs was also different, with the iX exhibiting the most instability on start-up. All linacs appear to converge to within 0.01 mm once stabilised. The TrueBeam machines tested had less stabilisation time than the Clinacs, with TrueBeam A showing no initial focal spot instability. This could simply be that the machine stabilised faster than the frame rate, or possibly that the machine performed well on the day of measurement.

The data was acquired at a dose rate of 600 MU/min. This corresponds to a delivery of 25 MU at 2.5 s stabilization time for the iX. The Trilogy delivers 10–30 MU depending on which energy and gantry angle is being used, and TrueBeam B delivers up to 10 MU. Sonke et al. [30] found the stabilization occurs after the delivery of 20 MU at dose rates between 350 MU/min and 500 MU/min on 5 Elekta Linacs and 2 Varian Clinacs. This corresponds to stabilization times of 2.4–3.4 s, which is consistent with results presented here.

The effects of focal spot instability results in a blurring of the source and an increase in the apparent source size, which in turn increases the geometric penumbra region, reducing treatment quality. The effect of this is negligible for high dose per beam treatments, or low dose rate treatments, where the source can stabilise before much of the treatment is delivered. The effect of beam holds in the treatment may require the beam to re-stabilise, reducing the quality of treatment. The size of this effect and its clinical implications are topics for further research.

The method can be used at any gantry angle due to the stability of the phantom, and is not limited to gantry 0° like previously proposed methods. The quick setup and delivery time make this test an effective tool for characterizing focal spot position and instability at multiple gantry angles during linac commissioning and annual QA. It can also be used to investigate trends in focal spot position and instability over the machines lifetime.

Phantomless methods such as the method proposed by Chojnowski et al. [28] and Barnes et al. [29] may be more suited to monthly QA at gantry 0°.

5. Conclusion

The method proposed has proven to be an effective tool in the localisation of the position of the focal spot relative to the collimator's axis of rotation (CAX) with a low uncertainty. Unlike previous methods, this method has been shown to work at any gantry angle due to the stability of the phantom.

The focal spot was shown to be unstable for the first 1–3 s, or 10–30 MU, of treatment before stabilising to within 0.01 mm from the mean position for the Varian Trilogy and Varian Clinac iX Linacs. One of the Varian TrueBeams showed less than 1 s of instability, with the second TrueBeam showing no initial instability. There were no trends observed between machines as to which gantry angle or beam energy had the most instability.

Declaration of Competing Interest

None

Acknowledgements

The authors of this paper would like to thank David J Cryer from the Department of Medical Technology and Physics, Sir Charles Gairdner Hospital, for the assistance manufacturing the phantom and running simulations to determine the phantom's stability. This work was partly supported by the Western Australia Department of Health, Australia (1089301 Merit Award fellowship) and Internationaliseringspuljen, Odence University Hospital, Odense, Denmark.

References

[1] Treuer H, et al. On isocentre adjustment and quality control in linear accelerator based radiosurgery with circular collimators and room lasers. Phys Med Biol 2000;45:2331–42. https://doi.org/10.1088/0031-9155/45/8/318.
[2] Chojnowski J, Gajewski R. An automatic method of the isocenter position

verification for micromultileaf collimator based radiosurgery system. Australas Phys Eng Sci Med 2010;34:15–21. https://doi.org/10.1007/s13246-010-0044-2.
[3] Rowshanfarzad P, et al. Verification of the linac isocenter for stereotactic radiosurgery using cine-EPID imaging and arc delivery. Med Phys 2011;38(7):3963–70. https://doi.org/10.1118/1.3597836.
[4] Dong L, et al. Verification of radiosurgery target point alignment with an electronic portal imaging device (EPID). Med Phys 1997;24:263–7. https://doi.org/10.1118/1.598070.
[5] Rowshanfarzad P, et al. Isocenter verification for linac-based stereotactic radiation therapy: review of principles and techniques. J Appl Clin Med Phys 2011;12(4):185–95. https://doi.org/10.1120/jacmp.v12i4.3645.
[6] D'Souza H, et al. Variation in the isocenter of a Philips linear accelerator (SL–20) used for stereotactic radiosurgery/stereotactic radiotherapy. Australas Radiol 1999;43:342–5. https://doi.org/10.1046/j.1440-1673.1999.433691.x.
[7] Skworcow P, et al. A new approach to quantify the mechanical and radiation isocentres of radiotherapy treatment machine gantries. Phys Med Biol 2007;52(23):7109–24. https://doi.org/10.1088/0031-9155/52/23/022.
[8] Riis HL, Zimmermann SJ, Hjelm-Hansen M. Gantry and isocenter displacements of a linear accelerator caused by an add-on micromultileaf collimator. Med Phys 2013;40(3). https://doi.org/10.1118/1.4789921.
[9] Rowshanfarzad P, et al. Investigation of the mechanical performance of Siemens linacs components during arc: gantry, MLC, and electronic portal imaging device. Med Devices (Auckl) 2015;2015(8):457–66. https://doi.org/10.2147/MDER.S89725.
[10] Winkler P, et al. Introducing a system for automated control of rotation axes, collimator and laser adjustment for a medical linear accelerator. Phys Med Biol 2003;48:1123–32. https://doi.org/10.1088/0031-9155/48/9/303.
[11] Rosca F, et al. An MLC-based linac QA procedure for the characterization of radiation isocenter and room lasers position. Med Phys 2006;33(6):1780–7. https://doi.org/10.1118/1.2198171.
[12] Woo MK, et al. Mechanical and radiation isocenter coincidence: an experience in linear accelerator alignment. Med Phys 1992;19:357–9. https://doi.org/10.1118/1.596866.
[13] Rowshanfarzad P, et al. Investigation of the sag in linac secondary collimator and MLC carriage during arc deliveries. Phys Med Biol 2012;57(12). https://doi.org/10.1088/0031-9155/57/12/N209.
[14] Baldwin Z, Fitchew R. The influence of focal spot size, shape, emission profile and position on field coverage in a Gulmay D3300 Kilovoltage X-ray therapy unit. Australas Phys Eng Sci Med 2014;37:515–23. https://doi.org/10.1007/s13246-014-0280-y.
[15] Nyiri BJ, Smale JR, Gerig LH. Two self-referencing metods for the measurement of beam spot position. Med Phys 2012;39(12):7635–43. https://doi.org/10.1118/1.4766270.
[16] Lutz WR, Larsen RD, Bjärngard BE. Beam alignment tests for therapy accelerators. Int J Radiat Oncol Biol Phys 1981;7(12):1727–31. https://doi.org/10.1016/0360-3016(81)90201-7.
[17] Yuen L, McLucas C. Investigation of X-ray focal spot alignment using a jig of novel design. Australas Phys Eng Sci Med 2017;40:455–61. https://doi.org/10.1007/s13246-017-0549-z.
[18] Klein EE, et al. Task Group 142 report: Quality assurance of medical accelerators. Med Phys 2009;36(9):4197–212. https://doi.org/10.1118/1.3190392.
[19] Tsai J-S, et al. The measurement of linear accelerator isocenter motion using a three-micrometer device and an adjustable pointer. Int J Radiation Oncology Biol Phys 1996;34(1):189–95. https://doi.org/10.1016/0360-3016(95)02085-3.
[20] Glide-Hurst C, et al. Commissioning of the Varian TrueBeam linear accelerator: a multi-institutional study. Med Phys 2013;40(3).. https://doi.org/10.1118/1.4790563.
[21] Depuydt T, et al. Computer-aided analysis of star shot films for high-accuracy radiation therapy treatment units. Phys Med Biol 2012;57:2997–3011. https://doi.org/10.1088/0031-9155/57/10/2997.
[22] González A, Castro I, Martnez J. A procedure to determine the radiation isocenter size in a linear accelerator. Med Phys 2004;31(6):1489–93. https://doi.org/10.1118/1.1755491.
[23] Denton TR, et al. Quantifying isocenter measurements to establish clinically meaningful thresholds. J Appl Clin Med Phys 2015;16(2):175–88. https://doi.org/10.1120/jacmp.v16i2.5183.
[24] Du W, Gao S. Measuring the wobble of radiation field centers during gantry rotation and collimator movement on a linear accelerator. Med Phys 2011;38(8):4575–8. https://doi.org/10.1118/1.3609098.
[25] Gao S, et al. Evaluation of IsoCal geometric calibration system for Varian linacs equipped with on-board imager and electronic portal imaging device imaging systems. J Appl Clin Med Phys 2014;15(3):p4688https://doi.org/10.1120/jacmp.v15i3.4688.
[26] Mayles P, Nahum A, Rosenwald JC. Handbook of Radiotherapy Physics: Theory and Practice. Taylor Francis Group: Hoboken; 2007.
[27] IEC. Radiotherapy Equipment – Coordinates, Movements and Scales. IEC 61217:2011, International Electrotechnical Commission 2011.
[28] Chojnowski JM, et al. Beam focal spot position: the forgotten linac QA parameter. An EPID-based phantomless method for routine Stereotactic linac QA. J Appl Clin Med Phy 2017;18(5):178–83. https://doi.org/10.1002/acm2.12147.
[29] Barnes MP, et al. A proposed method for linear accelerator photon beam steering using EPID. J Appl Clin Med Phys 2018;19(5):591–7. https://doi.org/10.1002/acm2.12419.
[30] Sonke JJ, Brand B, Herk MV. Focal spot motion of linear accelerators and its effect on portal image analysis. Med Phys 2003;30(6):1067–75. https://doi.org/10.1118/1.1576229.
[31] Varian TrueBeam Technical maintenance 2 training course lecture: Beam setup and Beam characteristics_SG Rev. 2.0.0. Varian Medical Systems, Palo Alto, CA, USA.
[32] Riis HL, Ebert MA, Rowshanfarzad P. Detection of the focal spot motion relative to the collimator axis of a linear accelerator under gantry rotation. Phys Med Biol 2018. https://doi.org/10.1088/1361-6560/aafa04.
[33] Barnes Michael P, Greer Peter B. Evaluation of the truebeam machine performance check (MPC) geometric checks for daily IGRT geometric accuracy quality assurance. J Appl Clin Med Phys 2017;18(3):200–6. https://doi.org/10.1002/acm2.12064.